

CFRP Retrofitting Schemes for Prestressed Concrete Box Beams for Highway Bridges

Herish A. Hussein¹ and Zia Razzaq²

¹ Old Dominion University

Received: 11 December 2016 Accepted: 1 January 2017 Published: 15 January 2017

Abstract

This paper investigates various retrofitting schemes for a prestressed concrete box beam using carbon fiber reinforced polymer (CFRP) sheets with the goal of increasing flexural strength. A simply-supported box beam is studied with a constant uniformly distributed load and three gradually increasing concentrated loads proportional to HS20 truck loading of the Association of State Highway and Transportation Officials (AASHTO). Various retrofitting schemes are considered each with single, double, and triple CFRP sheets, respectively, installed in high compression and tension regions. Cross-sectional nonlinear moment-curvature relations are developed and coupled with a finite-difference solution algorithm to predict load-deflection relations for both retrofitted and non-retrofitted box beams. The study identifies effective CFRP retrofitting schemes that result in a significant increase in the flexural strength of the prestressed concrete box beam.

Index terms— CFRP retrofitting, highway bridges, box beam, prestressed

etrofitting prestressed concrete beams to increase their strength is an evolving area of structural engineering research. Retrofitting with carbon fiber reinforced polymer (CFRP) strips or plates has been used in tensile regions of concrete beams [1][2][3]. CFRP retrofitting material is more advantageous than steel since it is non-corrosive, light-weight, easy to ship, available in practically any length, and easy to install [4][5][6]. It also exhibits superior fatigue resistance, low thermal expansion, and low relaxation [7][8][9]. Using CFRP laminar sheets on various parts of beams with high-strength adhesive epoxy can increase flexural strength and even support any damaged strands without having to demolish the affected areas [10][11][12]. Retrofitting tension regions in beams is of benefit not only to increase strength but also off-set weakness of concrete in tension, and protect prestressing strands from corrosion and vehicle impacts. This paper investigates the effectiveness of using CFRP retrofitting of prestressed concrete box beams in high tensile, compressive, and both tensile and compressive regions. Such retrofitting schemes can provide added strength for highway bridge girders.

Figure ?? shows a simply-supported prestressed concrete box beam used in highway bridges. The beam is subjected to AASHTO-type of loading in addition to the beam self-weight of 0.842 kips/ft. the external loading consists of a uniformly distributed load of 0.64 kips/ft., and concentrated loads 4P, 4P, and P as shown in Figure ?. The AASHTO loading is obtained if P=8 kips, however, in the present study, the value of P is gradually increased up to collapse condition in the presence of constant uniformly distributed loading. The Type BIII-48 box beam section has two rows of 7-wire ASTM Grade 270 ½ in. diameter strands as shown in Figure ?.

To demonstrate the effectiveness of CFRP retrofitting, an AASHTO Type BIII-48 box beam cross section [13] is adopted in the present study. Figure ??a shows the box beam cross section without retrofitting and is used as a reference beam section to determine the effectiveness of various retrofitting schemes. As shown in this figure, the prestressing is achieved with two rows of strands with 23 strands per row. Figures ??b and 2c show the box beam section retrofitted with a single 40 x 1/16 in. CFRP sheet, in tension and compression regions, respectively. Figure ??d shows the box beam with single CFRP sheets in both tension and compression regions. Figures ??e -2g show similar retrofitting schemes with double CFRP sheets while Figures ??h-2j show those with triple CFRP sheets. $\delta \text{ ???} \delta \text{ ???} \text{ ???} = \delta \text{ ???} \delta \text{ ???} \text{ ???} \text{ ' } [2(\text{? ? ? / ? ? ?}) (\text{? ? ? / ? ? ?}) 2](\mathbf{1})$

2 FIGURE 1: PRESTRESSED CONCRETE BOX BEAM WITH AASHTO-TYPE LOADING

The problem addressed in this study is to determine the effectiveness of various retrofitting schemes shown in Figures 2j through 2j. Abstract-This paper investigates various retrofitting schemes for a prestressed concrete box beam using carbon fiber reinforced polymer (CFRP) sheets with the goal of increasing flexural strength. A simply-supported box beam is studied with a constant uniformly distributed load and three gradually increasing concentrated loads proportional to HS20 truck loading of the Association of State Highway and Transportation Officials (AASHTO). Various retrofitting schemes are considered each with single, double, and triple CFRP sheets, respectively, installed in high compression and tension regions. Cross-sectional nonlinear moment-curvature relations are developed and coupled with a finite-difference solution algorithm to predict load-deflection relations for both retrofitted and non-retrofitted box beams. The study identifies effective CFRP retrofitting schemes that result in a significant increase in the flexural strength of the prestressed concrete box beam.

1 Introduction

where ϵ_c is the concrete strain, and ϵ_{cu} is the concrete strain at ultimate compression strength, δ is the deflection, σ_c is the concrete stress. The numerical results presented in this paper are based on a σ_{cu} value of 5.8 ksi and a concrete modulus of elasticity of 4,383 ksi. Each CFRP sheet used for retrofitting has a thickness of 1/16 in. and a width of 40 in. The Young's modulus of CFRP material is 22,000 ksi and it has an ultimate strength of 260 ksi. This is achieved by first formulating the nonlinear moment-curvature relations for the ten cross sections shown in Figure 2j followed by theoretical prediction of the load P versus maximum vertical deflection of the beam.

2 Figure 1: Prestressed concrete box beam with AASHTO-type loading

All moment-curvature relations presented in this paper are derived using 7-wire strands prestressed to a force F equal to 160 kips. In the analysis presented, the effects of keys and fillets on the moment-curvature relations for the cross sections in Figure 2j are considered negligible. This approximation results in only a 0.06% difference in the cross-sectional areas. Figure 2j shows the strain and stress distribution for a simply supported box beam with CFRP retrofitting at the bottom. In this figure, C_c , T_{ps} , and T_{CFRP} are the resultant concrete force, strand force, and CFRP force, respectively. The concrete force is found using: $C_c = \int \sigma_c dA$ (2)

where:

As seen in Figure 2j, the concrete strain, ϵ_c , can be expressed in terms of the curvature κ and distance y from neutral axis (NA): $\epsilon_c = \kappa y$ (3)

Substituting Equations 1 and 3 into Equation 2 results in $C_c = \int \sigma_c dA = \int \sigma_c b dy$ (4) which upon integration gives: $C_c = b \int \sigma_c dy$ (5)

In Figure 2j, X represents the distance of C_c from the NA, and is found using: $X = \frac{1}{C_c} \int y \sigma_c dA$ (6)

Using Equations 1, 5, and 6 gives: Moment-curvature relations are developed for seven different loading stages, namely, at zero external moment, zero strain in concrete at the c.g. of the strands, cracking moment, concrete strain reaching 0.001, 0.002, 0.00248, and 0.003 in./in. The linear portion of the moment-curvature relation is developed using elastic stress-strain distribution. The nonlinear portion of the $M-\kappa$ relation is developed by first assuming the top concrete strain and then determining the NA location iteratively until the axial force equilibrium is satisfied. The converged moment and curvature values are then found using the resulting forces and strain distribution. Using this procedure, the $M-\kappa$ curves are developed for the retrofitted cross sections shown in Figures 2j-2d, 2e-2g, and 2h-2j, respectively. These curves are presented in Figures 4, 5, and 6 including the curve for the non-retrofitted section shown in Figure 2a. $f = (0.12 \times 10^{-5} - 0.00008 \kappa) \times 10^{-5}$ (13) $g = (0.0004M - 13.7) \times 10^{-5}$ (14) $X = c/2 (8 \kappa^2 + 3 \kappa + 2) \times 10^{-5}$ (15) $h = M \times 2.935 \times 10^{-18}$ (16) $i = (0.035 \times 10^{-5} - 0.0001 \kappa) \times 10^{-5}$ (17) $j = (0.0003M - 9.5) \times 10^{-5}$ (18)

Equations 9 through 17 are obtained using Excel curve-fitting for use in load-deflection analysis based on finite-difference procedure. It is noteworthy that the same moment-curvature given by Equation 2 is found to be applicable to both of the box sections in Figures 2j and 2e. Also, in developing Equations 11, 13, and 16, the last point shown on the curves in Figures 4, 5, and 6 for sections 2c, 2f, and 2i, respectively, are excluded. However, these last points were included separately in the solution algorithm.

To predict the load-deflection relations for the prestressed box beam both without and with CFRP retrofitting, an algorithm is formulated based on the nonlinear moment curvature relations coupled with a finite-difference procedure. Figure 7 shows the finite-difference discretization along the longitudinal z axis of the box beam. The node numbers $i = 1, 2, \dots, N$ used in the finite-difference formulation are also shown in this figure, with nodes 0 and $N+1$ as the so-called phantom points. In this study, the segment length h is taken as $L/10$, where L is the total span of 95 ft. The curvature κ_i of the box beam at any node i can be expressed in the following central finite-difference form [15]: $\kappa_i = \frac{1}{h} \left(\frac{v_{i+1} - v_{i-1}}{2h} - \frac{v_{i+2} - v_{i-2}}{4h^2} \right)$ (18)

105 In this equation, V_i is the deflection at any node i . Applying Equation 18 at $i = 1, 2, \dots, N$, the following
 106 matrix expression is obtained: $[Q] \times \{V\} = h^2 \{ \dots \} \{V\}^T = \{V_0, V_2, V_3, \dots, V_{N-1}, V_{N+1}\}$

107 The curvature vector is defined by: $\{ \dots \}^T = \{ \dots, \dots, \dots, \dots, \dots \}$ (21)

108 In Equation ??9, the following zero deflection boundary conditions are incorporated: $V_1 = 0, V_N = 0$ ©

109 2017 Global Journals Inc. (US)

110 3 Global

111 $M_{IV} = 4878P - (4.279P \times z) + (570w \times z) - (w \times z^2 / 2)$ for 766 in. $z \leq 1140$ in (22c)

112 IV.

113 4 Solution Algorithm

114 where $[Q]$ is a $N \times N$ coefficient matrix, and $\{V\}$ is a deflection vector defined by: Year 2017 Based on the values
 115 found in $\{V\}$, the largest deflection is found to be at node 6 when $N = 11$ is used in the present study. Using
 116 this procedure, the loaddeflection curves for the retrofitted cross sections shown in Figures ??b-2d, 2e-2g, and
 117 2h-2j are developed and shown in Figures 8-10 including the curve for the nonretrofitted section shown in Figure
 118 ??a.

119 Table 1 presents a summary of the results based on a rigorous nonlinear analysis of the box beam shown in
 120 Figure ??. In this table, c_2 represents the location of the neutral axis at collapse. The values of the collapse
 121 load and the corresponding maximum bending moment are represented by P_{max} and M_{max} , respectively.
 122 When nondimensionalized using P_{max} and M_{max} values for the non-retrofitted box beam section 2a, they are
 123 entered as p_{max} and m_{max} values in this table. It is seen that the p_{max} values for various retrofitting schemes
 124 range from 1.05 to 1.52 showing that the retrofitting scheme using section 2j is the most effective of the ones
 125 investigated in this study. The range of m_{max} values is seen to be from 1.03 to 1.35. The second most effective
 126 retrofitting scheme corresponds to the section 2g providing a p_{max} value of 1.35.

127 Figure ??1 shows the relationships between box beam moment capacity and the CFRP thickness. The upper
 128 curve is for retrofitting with CFRP in both tension and compression, and the lower curve is when CFRP is used
 129 only in tension. A comparison of the two curves in this figure shows clearly that CFRP retrofitting is significantly
 130 more effective when used in both tension and compression regions.

131 5 Conclusions

132 The following conclusions are drawn from this study: 1. The use of a 3/16-inch thick CFRP retrofitting layer
 133 in both tension and compression regions resulted in the largest increase in the load carrying capacity of the box
 134 beam. 2. Retrofitting with CFRP simultaneously in both tension and compression regions is for more effective
 135 than retrofitting in just the tensile or the compressive region of the box beam. 3. Retrofitting with CFRP in
 136 tension only results in practically the same load carrying capacity of the box beam as that obtained with CFRP
 137 in compression only. The nonlinear analysis procedure presented is found to give rapid convergence for the box
 beam problem studied.

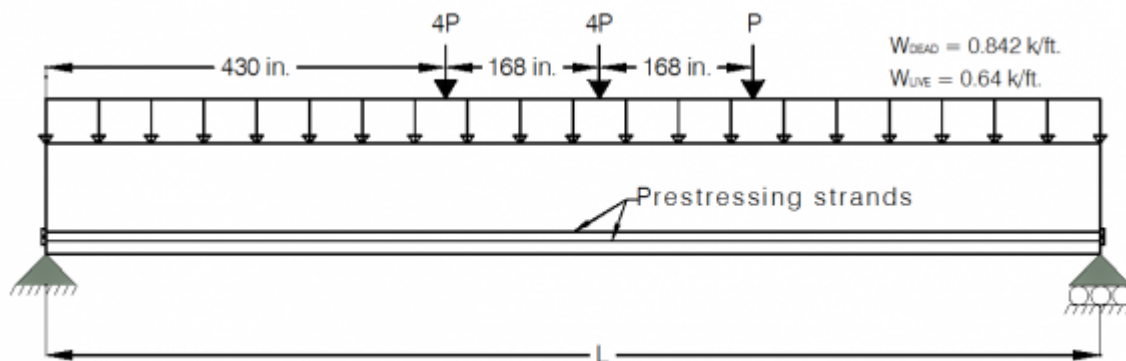


Figure 1:

138

¹Year 2017 E CFRP Retrofitting Schemes for Prestressed Concrete Box Beams for Highway Bridges © 2017 GlobalJournals Inc. (US)

²Year 2017

³© 2017 Global Journals Inc. (US)

5 CONCLUSIONS

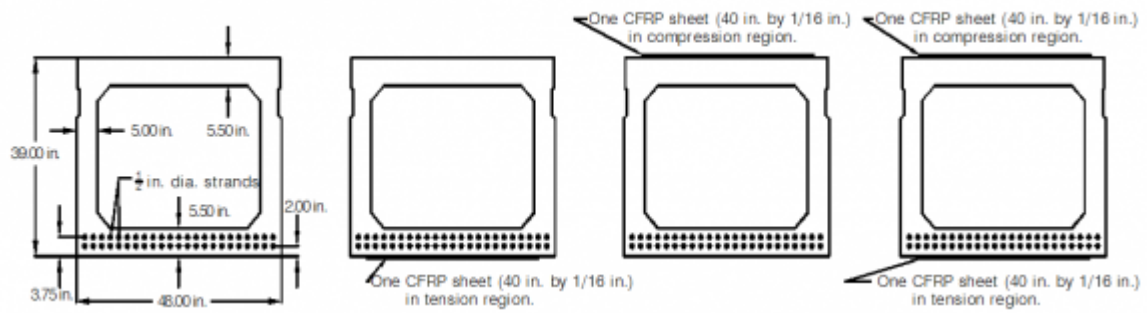
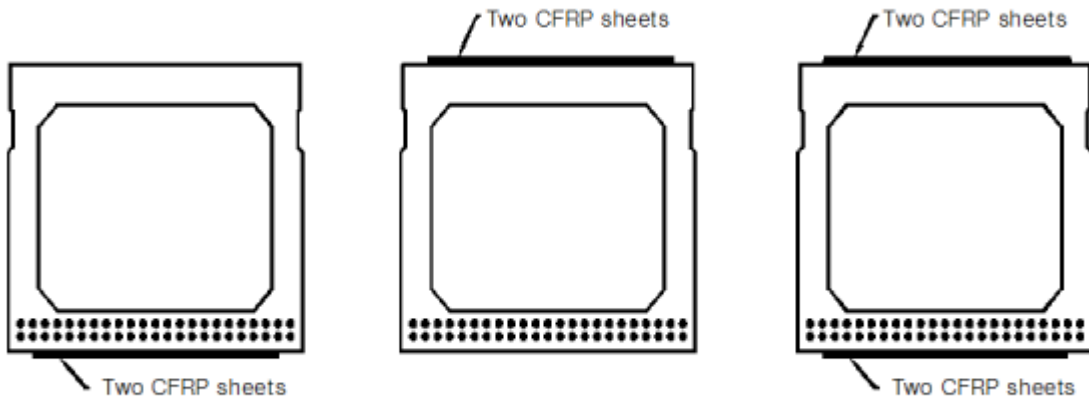
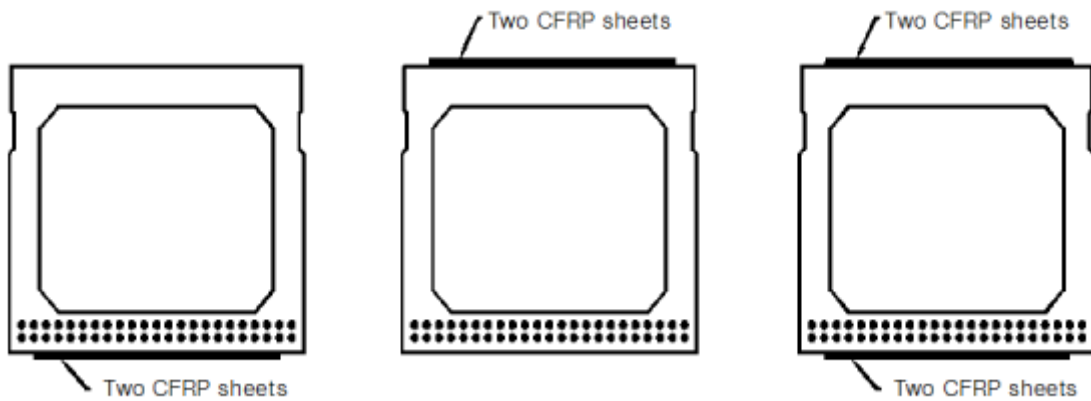


Figure 2:



23

Figure 3: Figure 2 :Figure 3 :



4

Figure 4: Figure 4 :

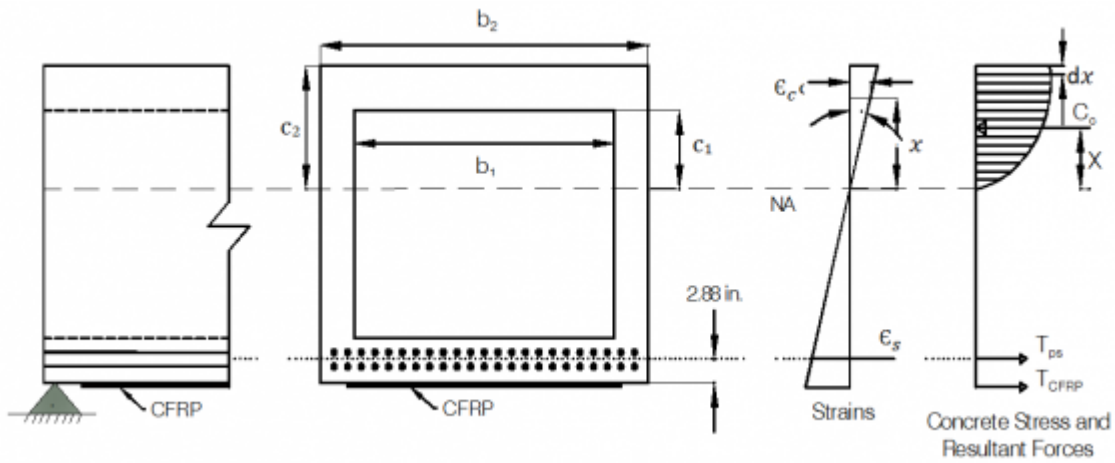
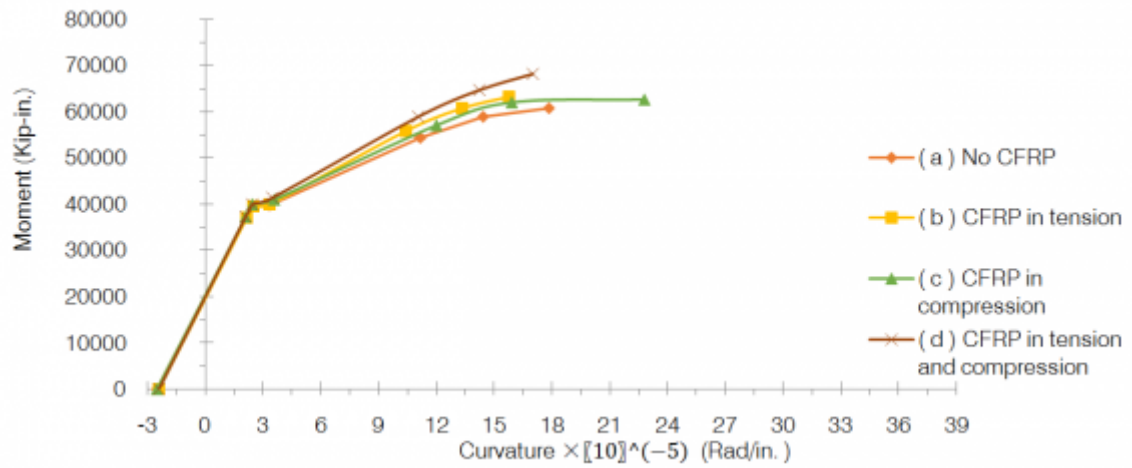
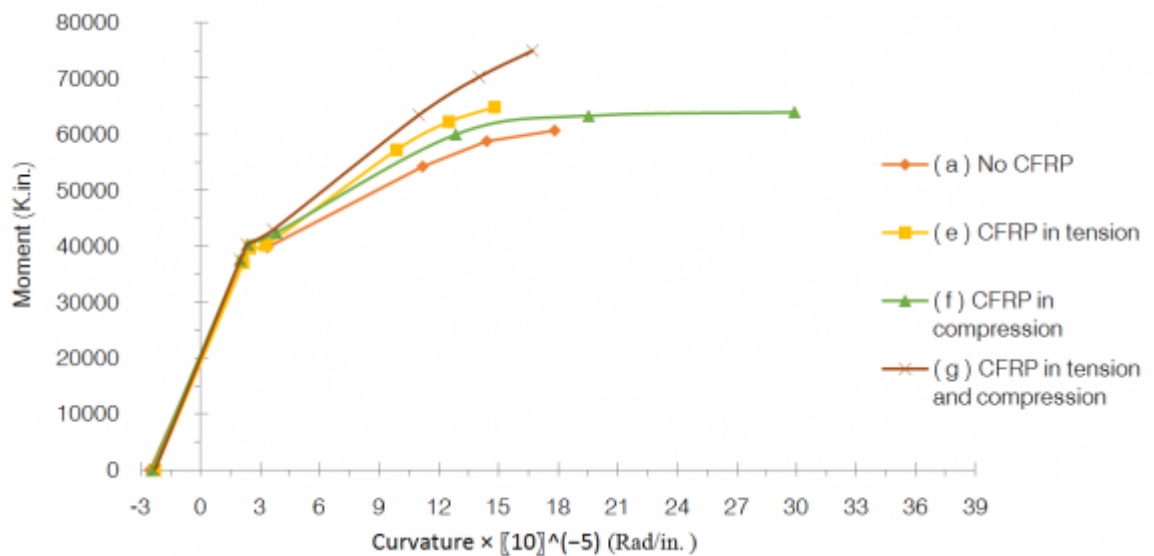


Figure 5:



5

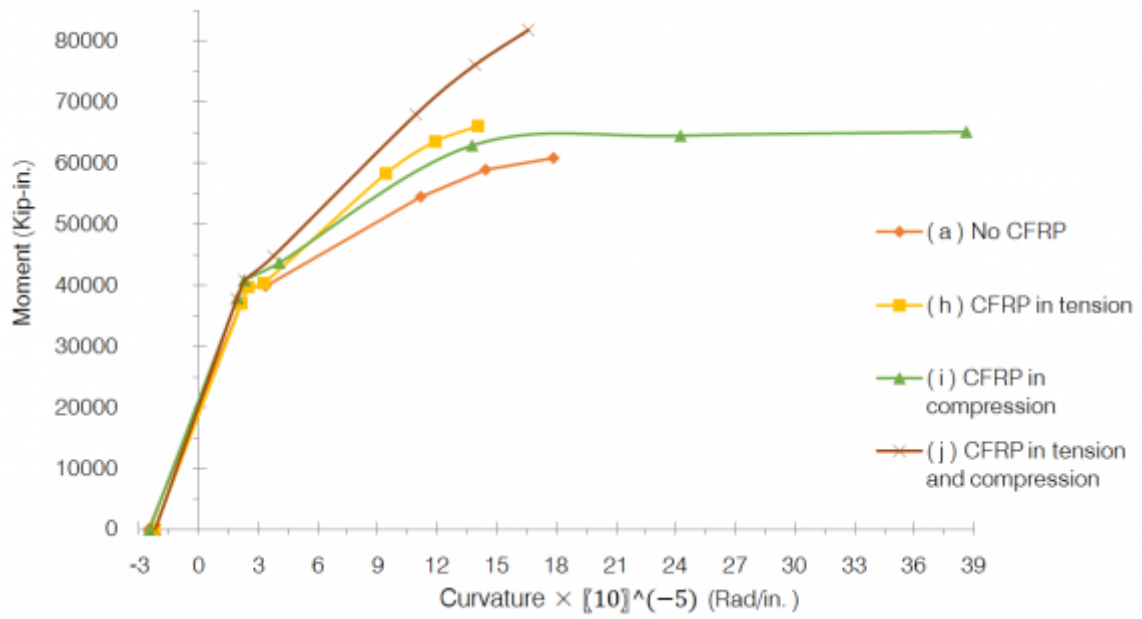
Figure 6: Figure 5 :



6510

Figure 7: Figure 6 : 5 (10)

5 CONCLUSIONS



7

Figure 8: Figure 7 :

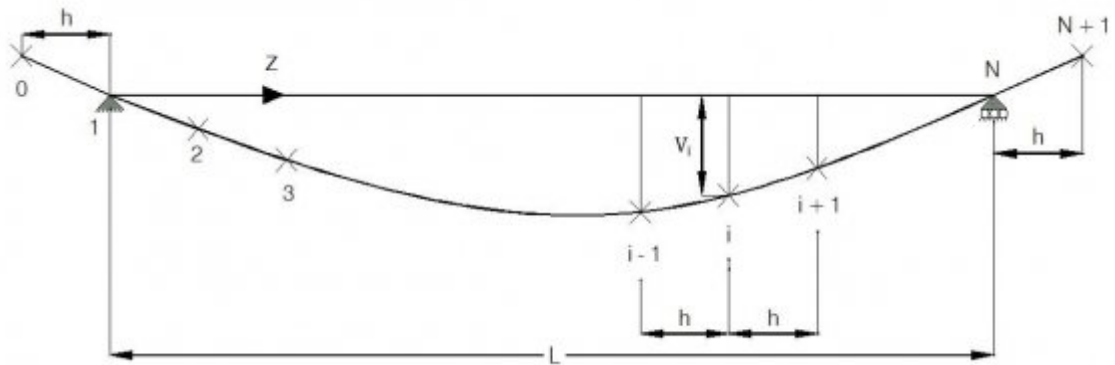
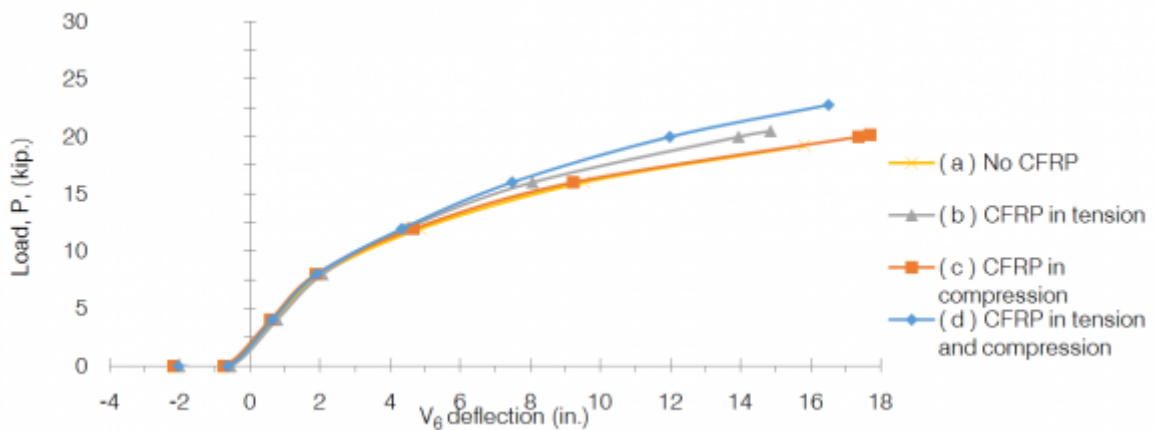
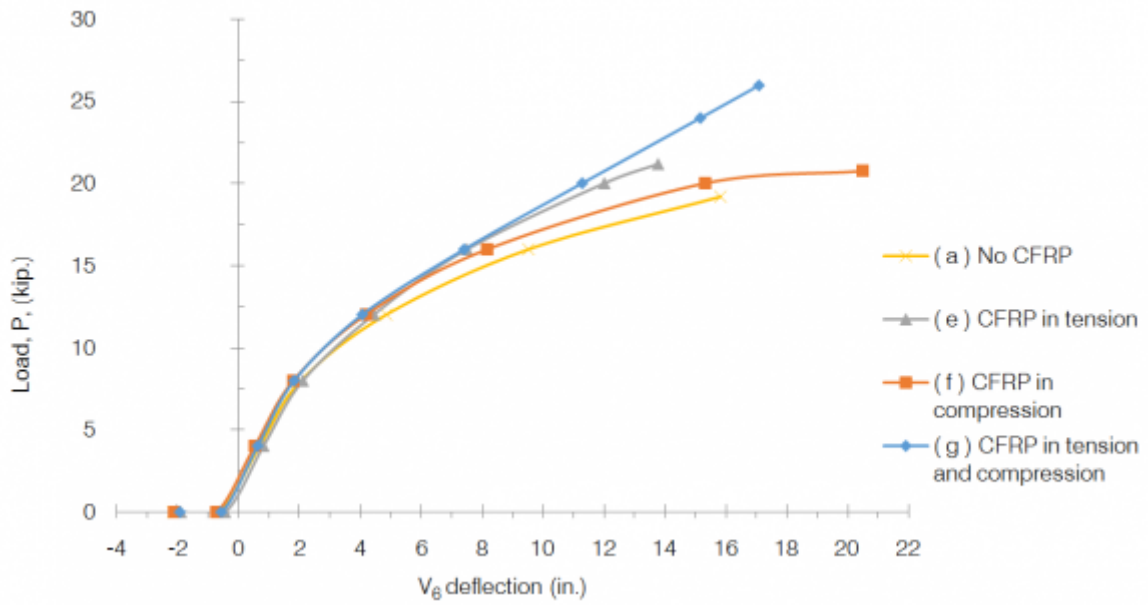


Figure 9: E



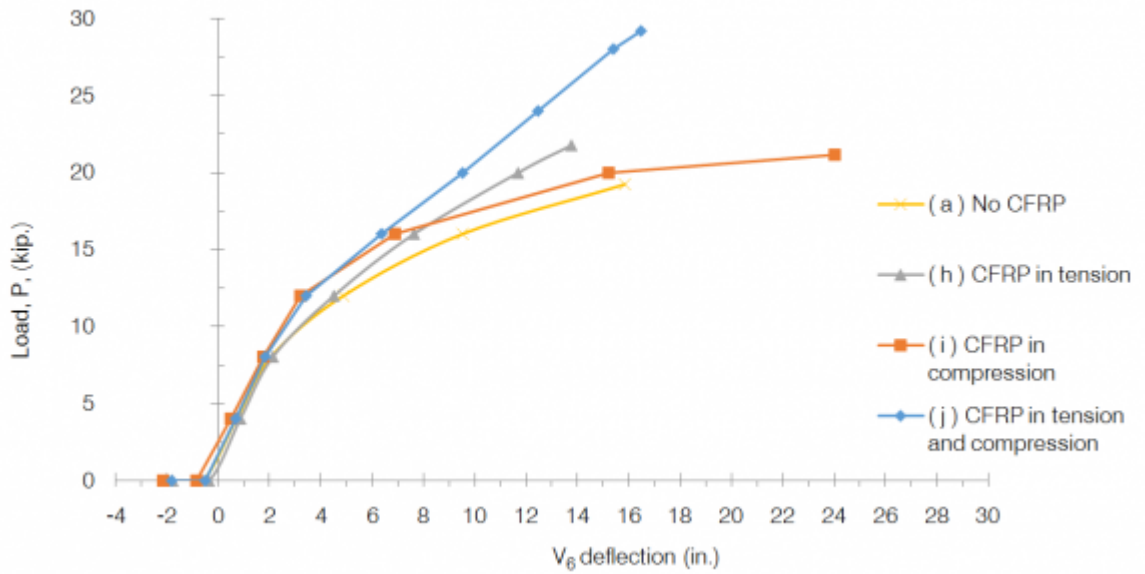
8

Figure 10: Figure 8 :



9

Figure 11: Figure 9 :



1011

Figure 12: Figure 10 :Figure 11 :

5 CONCLUSIONS

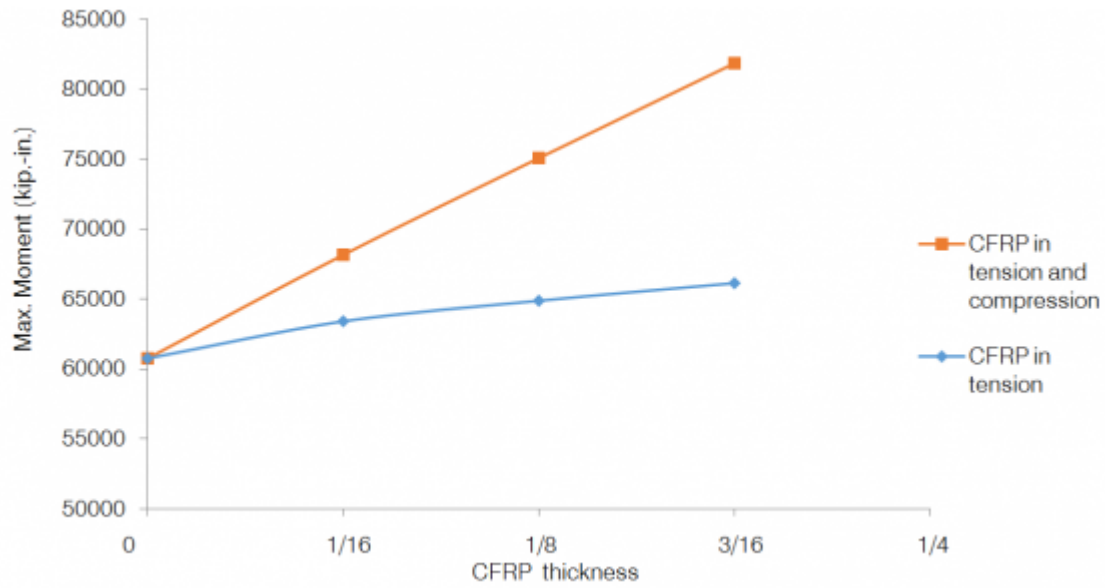


Figure 13:

1

Section (Figure 2)	c 2 (in.)	P max (kips)	p max	M max (kip-in.)	m max
2a	16.81	19.22	1.00	60749	1.00
2b	19.02	20.45	1.06	63364	1.04
2c	13.16	20.12	1.05	62657	1.03
2d	17.64	22.73	1.18	68175	1.12
2e	20.3	21.17	1.10	64876	1.07
2f	10.04	20.78	1.08	64058	1.05
2g	17.94	25.98	1.35	75069	1.23
2h	21.38	21.74	1.13	66098	1.09
2i	7.77	21.27	1.11	65088	1.07
2j	18.12	29.19	1.52	81852	1.45

VI.

Figure 14: Table 1 :

-
- 139 [Aashto and Lrfd ()] *American Association of State Highway and Transportation Officials, Aashto , Lrfd . 2014.*
140 Loose Leaf. (Bridge Design Specifications)
- 141 [Rosenboom and Rizkalla ()] ‘Behavior of Prestressed Concrete Strengthened with Various CFRP Systems
142 Subjected to Fatigue Loading’. O Rosenboom , S Rizkalla . *ASCE: Journal of Composites for Construction*
143 2006. (10) p. .
- 144 [Lin and Burns ()] *Design of prestressed concrete structures*, T Y Lin , N H Burns . 1981. John Wiley & Sons,
145 Incorporated, New Jersey.
- 146 [Kim et al. ()] ‘Ductility and Cracking Behavior of Prestressed Concrete Beams Strengthened with Prestressed
147 CFRP Sheets’. Y J Kim , S Chen , M F Green . *Journal of Composites for Construction* 2008. (12) p. .
- 148 [Aram et al. ()] ‘Effects of Gradually Anchored Prestressed CFRP Strips Bonded on Prestressed Concrete
149 Beams’. M Aram , C Czaderski , M Motavalli , M . *ASCE: Journal of Composites for Construction* 2008.
150 (12) p. .
- 151 [Reed and Peterman ()] ‘Evaluation of Prestressed Concrete Girders Strengthened with Carbon fiber reinforced
152 polymer Sheets’. C E Reed , R J Peterman . *Journal of Bridge Engineering* 2004. (9) p. .
- 153 [Ritchie et al. ()] ‘External reinforcement of concrete beams using fiber reinforced plastics’. P A Ritchie , D A
154 Thomas , L W Lu , G M Connelly . *ACI Structural Journal, No* 1991. 88 (4) p. .
- 155 [Kim et al. ()] ‘Flexural behavior of reinforced or prestressed concrete beams including strengthening with
156 prestressed carbon fiber reinforced polymer sheets’. Y J Kim , M F Green , R Wight . *Canadian Journal of*
157 *Civil Engineering* 2007. (34) p. .
- 158 [Rusinowski and Täljsten ()] ‘Intermediate Crack Induced Debonding in Concrete Beams Strengthened with
159 CFRP Plates’. P Rusinowski , B Täljsten . *Advances in Structural Engineering* 2009. (12) p. .
- 160 [Grace et al. ()] ‘Performance of an AASHTO Beam Bridge Prestressed with CFRP Tendons’. N Grace , E Jensen
161 , V Matsagar , P Penjendra . *Journal of Bridge Engineering* 2013. 18 (2) p. . (No.)
- 162 [Bennitz et al. ()] ‘Reinforced Concrete T-Beams Externally Prestressed with Unbonded Carbon Fiber-
163 Reinforced Polymer Tendons’. A Bennitz , J Schmidt , J Nilimaa , B Täljsten , P Goltermann , D Ravn
164 . *ACI Structural Journal* 2012. (109) p. .
- 165 [Burningham et al. ()] ‘Repair of Prestressed Concrete Beams with Damaged Steel Tendons Using Post-
166 Tensioned Carbon Fiber-Reinforced Polymer Rods’. C A Burningham , C P Pantelides , L D Reaveley .
167 *ACI Structural Journal* 2014. (111) p. .
- 168 [Chagnon and Massicotte ()] ‘Seismic retrofitting of rectangular bridge piers with CFRP’. N Chagnon , B
169 Massicotte . *Canada* 2005. p. .
- 170 [Petro] *Series of bridges in phoenix strengthened successfully*, S Petro . <http://www.gannettfleming.com>